

# Gas2, a Growth Arrest-specific Protein, Is a Component of the Microfilament Network System

Claudio Brancolini,\* Stefano Bottega,\* and Claudio Schneider\*†

\*International Center for Genetic Engineering and Biotechnology (I.C.G.E.B.), Padriciano 99 34012 Trieste, Italy; and  
†Istituto di Biologia, Facoltà di Medicina e Chirurgia via Gervasutta 48, Università di Udine, 33100 Udine, Italy

**Abstract.** In this report we analyze the protein product of a growth arrest-specific gene, *gas2*, by means of an affinity-purified antibody raised against the protein produced in bacteria. The regulation of Gas2 biosynthesis reflects the pattern of mRNA expression (Schneider, C., R. King, and L. Philipson. 1988. *Cell*. 54:787-793): its relative level is tightly associated with growth arrest. Gas2 seems to be regulated also at the posttranslational level via a phosphorylation mechanism. Gas2 is well conserved during the evolution with the same apparent molecular mass (36 kD) be-

tween mouse and human.

We also demonstrate that Gas2 is a component of the microfilament system. It colocalizes with actin fiber, at the cell border and also along the stress fiber, in growth-arrested NIH 3T3 cells. The pattern of distribution, detected in arrested cells, can also be observed in growing cells when they are microinjected with the purified GST-Gas2 protein.

In none of the analyzed oncogene-transformed NIH 3T3 cell lines was Gas2 expression induced under serum starvation.

To gain insight about the mechanism that controls growth arrest in mammalian cells, we have cloned a set of genes that are highly expressed during growth arrest mediated by either serum starvation or density-dependent inhibition in NIH 3T3 mouse fibroblasts (30).

These genes have been called growth arrest specific (*gas*)<sup>1</sup>; their expression is downregulated during the first hours after serum induction of arrested NIH 3T3 cells. The same striking regulation of *gas* gene expression in relation to growth arrest appears, at least in one instance, to hold true also in vivo. The expression of the rat homologue of *gas3* gene, (20) highly homologous to a membrane protein found as a myelin component (16), is in fact strongly downregulated during the cellular response to nerve injury, when Schwann cells proliferation starts (41).

To understand the functional role of *gas* genes in the maintenance and induction of growth arrest we have undertaken the characterization of their protein products.

In this paper we report on the product of *gas2*; using a specific antibody it is shown that the regulation of its biosynthesis exactly reflects the pattern of mRNA expression. The protein seems to be regulated also at the posttranslational level via a phosphorylation mechanism. By double immunofluorescence analysis it colocalizes with actin filaments, its distribution being prevalent at the cell border, but it is also detectable along the stress fibers.

We demonstrate that the purified fusion protein GST-Gas2, when microinjected in growing cells, is localized in the microfilament apparatus, both at the cell border and at the level of stress fibers, in a pattern similar to endogenous Gas2 in arrested cells. Moreover, when a microvillar appara-

tus is present in the microinjected cells, GST-Gas2 becomes most intensely localized in this region. It is well known that distinct regional levels of organization exist within the microfilament network: (a) at the level of the leading edge where ruffles and microspikes are present in tight connection with the plasma membrane; (b) at the level of stress fibers all along the cellular length; (c) at the ventral face of the cells in the adherent junctions; or (d) in microvillar structures at the dorsal side of the cells.

The local differences of microfilaments system present in these cellular loci can be achieved by different rates of actin polymerization (25) and/or by the specific compartmentalization of actin-binding proteins (ABPs) or microfilament-associated proteins (for review see 4, 22, 33, 34). For example, in cultured fibroblasts myosin is associated with stress fibers but is less abundant in the microfilament's rich ruffling membrane (39). On the contrary, fimbrin is largely absent in stress fibers (3), but present in the ruffling membrane, while vinculin and tensin are mainly present in adherent junctions (4, 9). Other organizing proteins seem to be more promiscuous such as  $\alpha$ -actinin (26, 40), which can be detected both in adherent junctions and along the stress fibers.

We have no results bearing on the role that Gas2 has in microfilament organization, or in what kind of structure it might serve as a component. The fact that its expression is induced in growth arrest may constitute a level of regulation whereby at least one unit of the microfilament system might be involved in a specific growth arrest organization.

1. *Abbreviations used in this paper:* ABP, actin-binding protein; BrdUrd, bromodeoxyuridine; *gas*, growth arrest-specific gene; Gas, growth arrest-specific protein; GST, glutathione-s-transferase.

## Materials and Methods

### Cell Lines and Culture Conditions

NIH 3T3 were routinely cultured in DME with 10% FCS. In each experiment  $10^5$  cells/ml were seeded in 35-mm Petri dishes.

For serum starvation, medium was changed to 0.5% FCS when cells were subconfluent, and cells were then left in this medium for 48 h. Under these conditions, incubation with 50  $\mu$ M bromodeoxyuridine (BrdUrd) for an additional 3 h resulted in labeling of <3% of the nuclei. For induction of DNA synthesis, fresh medium containing 20% FCS was added to the arrested cells. 18 h after activation with serum, a 2-h pulse of BrdUrd, resulted in ~90% of the positive nuclei. For density-dependent inhibition, cells were plated at  $10^4$ /cm<sup>2</sup> in 10% FCS. 12 h after plating (considered as the starting point for growing cells), the medium was changed every 2 d. After 4 d in culture, incubation with BrdUrd for 2 h resulted in <5% incorporation in the nuclei. Exponentially growing cells are cells cultured for 24 h in 10% FCS. After this time, incubation with BrdUrd for 2 h resulted in 60% incorporation.

NIH 3T3 transformed with *v-ras*, *v-myc*, and *v-src* (2) were kindly provided by Prof. F. Taro' (University of Rome, Italy). NIH 3T3 transformed with *v-fos* were kindly provided by Prof. R. Muller (Institut für Molekular Biologie und Tumorforschung, Marburg, Germany) (2).

### DNA Synthesis Assay

Cells grown on coverslips in the same culture dishes from which protein extracts were prepared were incubated for 2 h in the presence of 50  $\mu$ M BrdUrd. After this time cells were fixed for 20 min in 3% paraformaldehyde and permeabilized with 0.1% Triton X-100. DNA was then denatured by treatment for 10 s with 50 mM NaOH. After neutralization the coverslips were incubated with mouse mAb against BrdUrd for 1 h at 37°C. The second antibody was TRITC-conjugated rabbit anti-mouse Ig antibodies. Total nuclei were visualized with Hoechst 33342 (1  $\mu$ g/ml). The percentage of cells in S phase was calculated as the ratio between positive for TRITC and total cells (Hoechst 33342 stained).

### gas2 Expression in *E. coli*

The *gas2* expression vector was constructed by digesting *gas2* cDNA with endonuclease HincII (fragment from nucleotide 378 to 1511). BamHI adaptors were ligated to the recovered fragment inserted into BamHI site of pAR 3040 vector which carries the promoter of the  $\Psi$  10 gene of T7 bacteriophage (35). Expression of T7 RNA polymerase was performed by infection of the host cells (*E. coli* bacterial strain Q 358) with bacteriophage  $\lambda\Phi$ CEG carrying bacteriophage T7 gene 1 with a multiplicity of infection of five to seven infectious phage particles per cell.

Bacteria containing the plasmid pAR3040/*gas2* were grown to saturation in LB medium supplemented with ampicillin (50  $\mu$ g/ml) and maltose (0.02%). The bacteria were diluted 1/100 in the same medium and grown to an optical density at 550 nm of 0.6–0.8. The expression of the T7 RNA polymerase was then induced by infection with the bacterial phage  $\lambda\Phi$ CEG.

The cultures were incubated for a further 3 h, and bacteria were collected and lysed as previously described (23). Under these conditions the Gas2 fusion protein can be isolated as inclusion bodies. These granules were separated from the cell debris by centrifugation.

The pellets were washed once and dissolved in sample buffer (2% SDS, 100 mM DTT, 60 mM Tris, pH 6.8) by boiling for 10 min. These samples were run on a preparative polyacrylamide gel and stained with Coomassie blue in water (0.05%) (13). The band corresponding to the Gas2 fusion product was excised and the protein electroeluted as described (13) and used to immunize rabbits.

To construct the GST-Gas2 fusion protein, oligonucleotides containing BamHI and HindIII sites were used to generate a polymerase chain reaction fragment of the complete *gas2* ORF, which was cloned in pGEX3 vector (32). The fusion protein was expressed in *E. coli* JM 101 bacterial cells. For purification, 1 liter of culture was grown to an absorbance A<sub>600</sub> of 0.4, induced for 3 h with 0.2 mM IPTG. The culture was then resuspended in 25 ml of buffer A (PBS, 0.5% CHAPS) and subjected to mild sonication. The clarified extract was incubated with 1 ml glutathione-Sepharose beads (Pharmacia Fine Chemicals, Piscataway, NJ) previously washed in buffer A, for 1 h at 4°C in a rotating platform. The beads were subsequently washed with buffer A followed by buffer B (0.4 M NaCl) and finally PBS. Bound protein was eluted by two 5-min incubations with 1 ml 50 mM Tris containing 5 mM glutathione (reduced, freshly prepared). Proteins for microinjection was dialyzed against 100 mM KCl.

### Affinity-purified Polyclonal Antibody Preparation

Rabbits were injected with 200  $\mu$ g purified bacterial Gas2 protein mixed with complete Freund's adjuvant. Subsequently they were injected with the same amount of protein in incomplete Freund's adjuvant every 3 wk for 2 mo.

For the affinity purification of the antibodies, 0.6 mg of purified bacterial Gas2 protein was covalently coupled to Affi-Prep 10 support (Bio-Rad Laboratories, Cambridge, MA). 1 ml of immune serum, diluted 10 times in 0.1% Triton X-100, 50 mM Tris, pH 8, 100 mM NaCl, was incubated batchwise with the affinity matrix preequilibrated in the same buffer.

After overnight incubation at 4°C, the matrix was poured in a column and washed with 50 vol column of the same buffer. Antibodies were eluted with 400  $\mu$ l of 0.2 M Glycine HCl, pH 2.8, and the fractions were neutralized with 50  $\mu$ l of 2 M Tris, pH 8.

### In Vitro Expression of *gas2*

To express cDNA of *gas2* in vitro, linearized plasmid was transcribed with T7 polymerase (Promega Biotec, Madison, WI) in the presence of 7mGpppG CAP (Pharmacia Fine Chemicals).

500 ng of the generated RNA was translated in rabbit reticulocyte extract containing [<sup>35</sup>S]methionine, as recommended by Novogene (Madison, WI).

For immunoprecipitation, 2  $\mu$ l of reticulocyte translation mixture was mixed with 0.1 ml of the NP-40 buffer (50 mM TEA, pH 7.5, 0.1% NP-40, 150 mM NaCl) and incubated for 30 min on ice with anti-Gas2 antibodies. After this time, 50  $\mu$ l of (10% wt/vol) suspension of protein A-Sepharose (Pharmacia Fine Chemicals) was added and the incubation was prolonged for 30 min at 4°C by rocking. After three washes with the NP-40 buffer the immunocomplex was resolved on SDS-PAGE.

### Immunoblotting

Preparation of cellular or organ extracts was performed by adding 10 vol of sample buffer (2% SDS, 100 mM DTT, 60 mM Tris, pH 6.8), which was vigorously mixed and boiled for 5 min. Before performing the final SDS-PAGE for the blot, the protein extracts were checked for equal amounts on separate gel stained by Coomassie blue. Proteins were transferred to 0.2- $\mu$ m pore sized nitrocellulose (Schleicher & Schuell, Dassel, Germany) using a semi-dry blotting apparatus (Bio-Rad Laboratories, Cambridge, MA) (transfer buffer: 20% methanol, 48 mM Tris, 39 mM glycine, and 1.3 mM SDS). After staining with Ponceau S, the nitrocellulose sheets were saturated for 2 h in Blotto-Tween 20 (13) (50 mM Tris-HCl, pH 7.5, 200 mM NaCl, 5% nonfat dry milk, and 0.1% Tween 20) and incubated overnight at room temperature with 1  $\mu$ g/ml of anti-Gas2 affinity-purified antibodies in Blotto-Tween 20 or with 1/500 dilution of antivimentin or antitubulin ascites fluids. After incubation, the nitrocellulose sheets were rinsed three times with Blotto-Tween 20 and reacted with alkaline phosphatase-conjugated sheep antirabbit (Dako Corp., Santa Barbara, CA) or goat antimouse (ICN Pharmaceuticals, Inc., Irvine, CA) for 1 h at room temperature. The blot was then washed four times in Blotto-Tween 20, rinsed in 100 mM Tris-HCl, pH 9.5, 100 mM NaCl, 5 mM MgCl<sub>2</sub>, and developed in the same buffer containing 0.3 mg/ml *p*-nitro blue tetrazolium chloride and 0.15 mg/ml 5-bromo-4-chloro-3-indoyl phosphate, *p*-toluidine salt.

### Immunoprecipitation

Cells growing in 35-mm petri dishes were labeled for the appropriate times in 1 ml of DME methionine-free 10% FCS when needed, containing 150  $\mu$ Ci/ml [<sup>35</sup>S]methionine (Amersham Corp., Arlington Heights, IL; 1,000 Ci/mmol; 1Ci = 37 GBq).

Cell monolayers were lysed with 0.5 ml of (100 mM NaCl, 50 mM TEA, pH 7.5, 0.8% SDS) lysis buffer on ice and then boiled for 4 min. After boiling 0.5 ml of SDS-quenching buffer (100 mM NaCl, 50 mM TEA, pH 7.5, 4% Triton X-100) was added containing (final concentration) 1 mM PMSF and 10  $\mu$ g/ml each of aprotinin, leupeptin, antipain, and pepstatin. (In some cases Triton X-100 lysis buffer was used [0.1% Triton X-100, 100 mM NaCl, 50 mM TEA].) The lysates were cleared by centrifugation for 2 min. The supernatants were incubated with 20  $\mu$ l of normal rabbit serum for 1 h on ice and transferred to a new Eppendorf tube containing 20  $\mu$ l wet volume pellet of prewashed Staph A. After resuspension of the Staph A., the lysates were incubated by continuous rocking at 4°C for 30 min and then centrifuged for 2 min in an Eppendorf centrifuge. This was repeated and the lysates were centrifuged for 10 min: the resulting supernatants were then used for immunoprecipitation. These lysates were incubated with the affinity-purified anti-GAS2 antibody for 3 h at 4°C with rocking. Finally,

80  $\mu$ l of protein A-Sepharose (10% wt/vol) suspension was added and the incubation was continued for 1/2 h by rocking at 4°C. Protein A-Sepharose was recovered by centrifugation, washed three times in Triton X-100 lysis buffer and finally resuspended in sample buffer. Immune complexes were released by boiling for 5 min.

For  $^{32}$ P labeling, NIH 3T3 cells were cultured for 40 h in 0.5% FCS; after this time phosphate-free medium containing 0.25 mCi/ml  $^{32}$ P and 0.5% FCS was added and left for a further 8 h. At the end of the labeling period they were either stimulated by addition of 20% FCS (activated cells) or left in the same labeling medium (resting cells) for 3 h.

### Immunofluorescence Microscopy

For indirect immunofluorescence microscopy of cultured cells, the cells on coverslips were fixed with 3% paraformaldehyde in PBS for 20 min at room temperature. The fixed cells were permeabilized with 0.1% Triton-X 100 in PBS for 5 min and then washed with PBS/0.1 M Glycine, pH 7.5. The samples were treated with the first antibody (anti-Gas2 diluted in PBS 3% BSA) for 1 h in a moist chamber at 37°C. They were then washed with PBS three times, followed by incubation with antirabbit biotinylated second antibody (Dako Corp.) for 1 h at 37°C. The immunocomplexes were visualized by incubation with rhodamine-conjugated streptavidin (Jackson Laboratory, Bar Harbor, ME). For the detection of actin filaments, FITC-phalloidin (Sigma Chemical Co., St. Louis, MO) was used. In the same experiments cells were treated before fixation with extraction buffer (2 mM MgCl<sub>2</sub>, 150 mM KCl, 20 mM TEA, 0.1% Triton X-100) for 2 min in ice. Anti-GST antibodies and F-actin were visualized using antirabbit FITC-conjugated (Dako Corp.) and TRITC-phalloidin (Sigma Chemical Co.), respectively. A Zeiss microscope was used for all the analysis with the following set of filters: rhodamine and (BP546, FT580, LP 590) fluoresceine (450-490, FT 510, LP520).

### Microinjection

GST-Gas2 fusion protein was microinjected at the concentration of 4 mg/ml

in exponentially growing cells using AIS system (Zeiss) as described elsewhere (27). Cells were fixed and processed for immunofluorescence 1 h later.

## Results

### Affinity-purified Polyclonal Antibody Recognizes the Protein Product (Gas2) of the *gas2* Gene

The growth arrest-specific gene (*gas2*) has been previously characterized at the structural and expressional level (30). To analyze the protein product of the *gas2* gene we immunized a rabbit with the *E. coli* expressed Gas2 protein. The antiserum was further purified on a Gas2 affinity column and initially used to compare the immunoprecipitation products from whole cell lysates of [ $^{35}$ S]methionine-labeled NIH 3T3 cells (Fig. 1 a, lane 5), with the immunoprecipitation product obtained from in vitro transcription/translation of *gas2* cDNA (Fig. 1 a, lane 4).

The primary translation product of *gas2* cDNA (Fig. 1 a, lane 2) is recognized by the antibody (Fig. 1 a, lane 4) and appears to have the same size (apparent molecular mass ~36 kD) as the polypeptide immunoprecipitated from growth-arrested NIH 3T3 cell lysate (Fig. 1 a, lane 5).

The expression of *gas2* mRNA is abundant at growth arrest induced by either serum starvation or saturation density (30). Furthermore, it becomes downregulated when arrested cells are reintroduced into cycle. We therefore examined first if the protein was similarly controlled.

Exponentially growing (Fig. 1 b, lanes 1 and 3) growth ar-

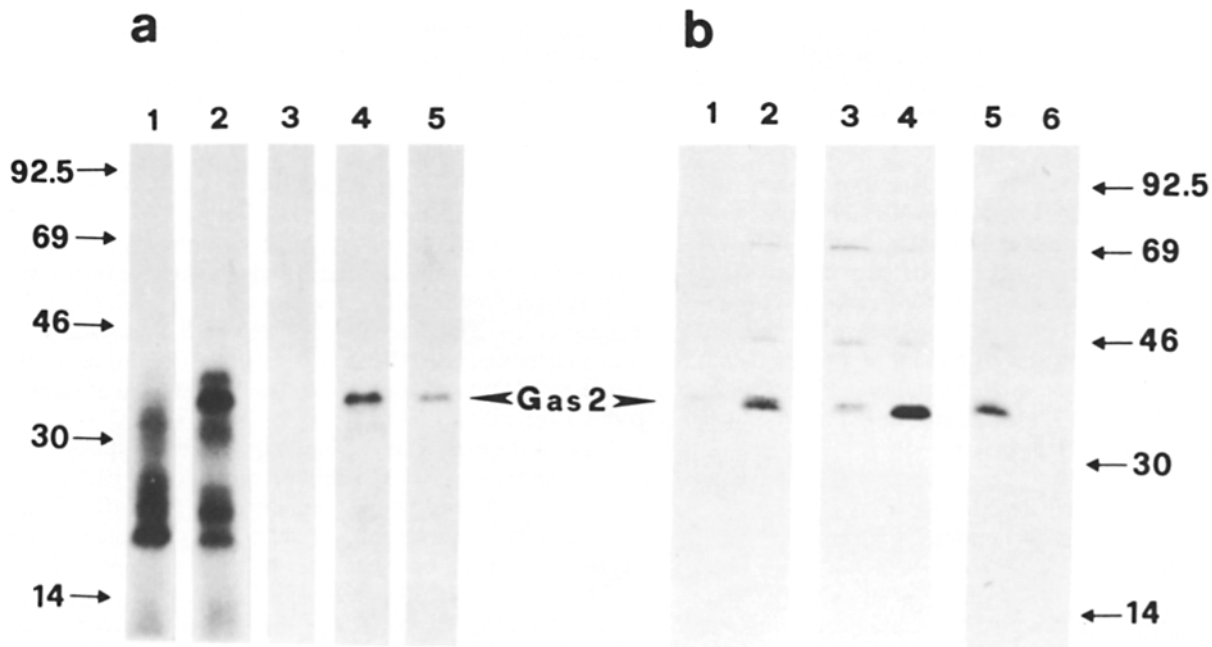


**Figure 1.** Immunoprecipitation analysis of Gas2. (a) (lane 1) Mock translation; (lane 2) in vitro translation of *gas2* mRNA; (lane 3) immunoprecipitation of mock translation; (lane 4) immunoprecipitation of the in vitro-translated product of *gas2* gene; (lane 5) immunoprecipitation of Gas2 from serum-starved cellular lysates after [ $^{35}$ S]methionine in vivo labeling. (b) Immunoprecipitation analysis of Gas2 under different growth conditions of NIH 3T3 cells. Exponentially growing cells, 24 h after seeding in 10% FCS (lane 1) and serum-starved cells, 48 h in 0.5% FCS (lane 2) were labeled for 3 h with [ $^{35}$ S]methionine. Equal numbers of TCA precipitable cpm from the respective lysates were processed for immunoprecipitation. Exponentially growing cells, 24 h after seeding in 10% FCS (lane 3) and density-dependent, growth-inhibited NIH 3T3 cells, 8 d after seeding in 10% FCS (lane 4) were labeled for 3 h with [ $^{35}$ S]methionine. Equal numbers of TCA precipitable cpm from the respective lysates were processed for immunoprecipitation. Serum-starved NIH 3T3 cells, 48 h in 0.5% FCS (lane 5) and serum-starved cells followed by 6 h of incubation with 20% FCS (lane 6) were labeled for 3 h with [ $^{35}$ S]methionine. Equal numbers of TCA precipitable cpm from the respective lysates were processed for immunoprecipitation.

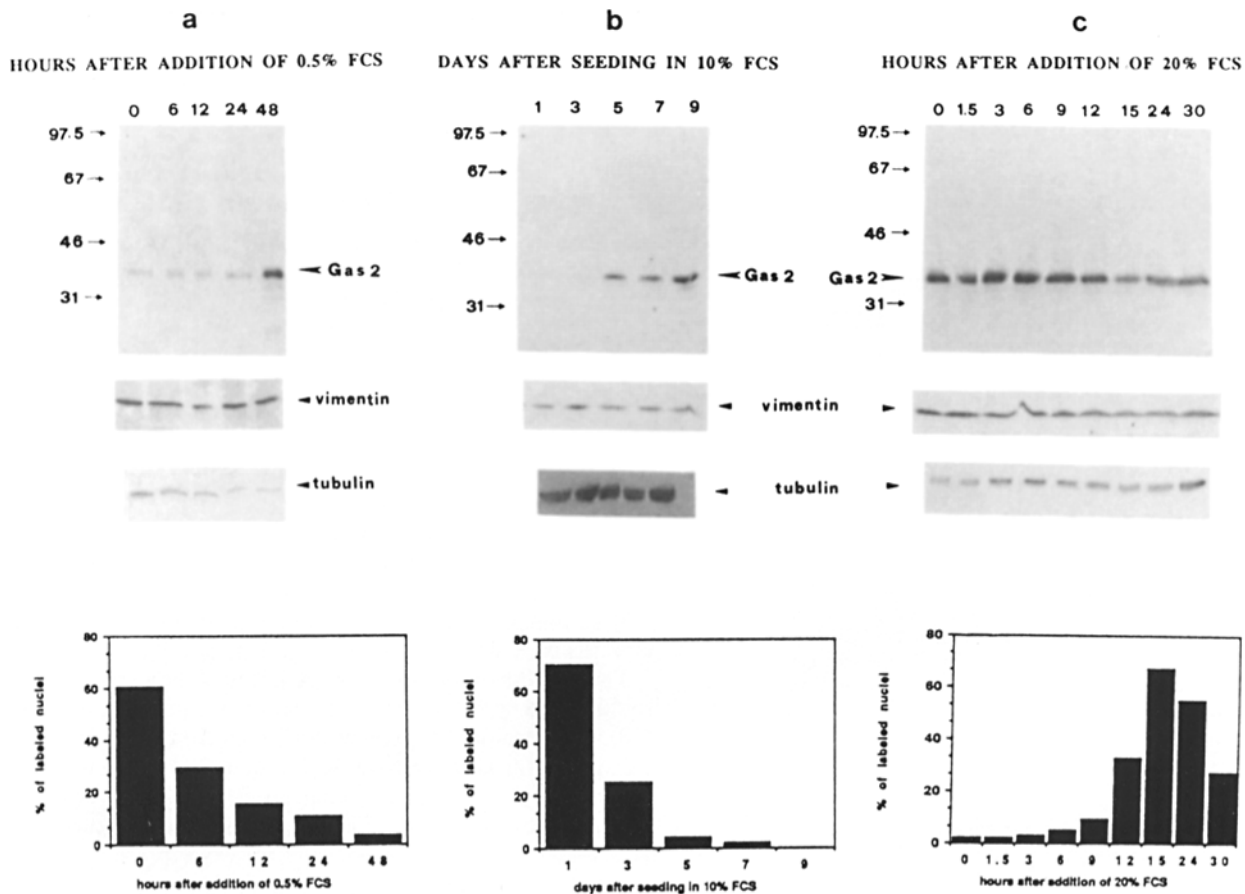


**Figure 2.** Western blot analysis of Gas2 expression. Proteins were extracted from: (a) actively growing NIH 3T3 cells and various times after serum starvation; (b) exponentially growing NIH 3T3 cells various days after cells seeding; and (c) from serum-starved NIH 3T3 cells various hours after 20% addition. Immunodecorations were performed with anti-Gas2, antivimentin, and antitubulin antibodies. BrdUrd incorporation is shown in diagram analysis.

rested by serum starvation (Fig. 1 b, lane 2) or by density-dependent inhibition (Fig. 1 b, lane 4) NIH 3T3 cells were labeled for 3 h with [<sup>35</sup>S]methionine. After cell lysis equal numbers of cpm were immunoprecipitated with anti-Gas2 antibody. Growth arrest induces in both cases a clear increase in the level of Gas2 protein. Moreover, when cells are growth arrested by serum starvation and reintroduced into a synchronous cell division cycle by addition of 20% FCS, the biosynthesis of Gas2 is clearly downregulated 6 h after serum stimulation (Fig. 1 b, lane 6).

#### **Analysis of Gas2 Expression under Different Growth Conditions**

To study the steady-state expression of Gas2 during different growth conditions we performed Western immunoblot analyses. Equal amounts of extracted proteins were loaded for each time point (as assessed by Coomassie blue staining of separate gels). Fig. 2 a shows the level of Gas2 expression after various times of serum deprivation of exponentially growing NIH 3T3 cells. Cells were shifted to 0.5% FCS 24 h after seeding in 10% FCS.

Gas2 is detectable in all lanes as a 36-kD band; in accordance with the previous analysis its level is lower in exponentially growing cells and remains low during the first 24 h of

serum deprivation but increases dramatically, between 24 and 48 h of serum starvation.

The same lysates were also probed with mAbs against vimentin used as invariant control and with a polyclonal antibody against tubulin whose level is known to be cell cycle regulated (29). The percentage of cells in S phase was also measured by analyzing the incorporation of BrdUrd in newly synthesized DNA on coverslips for each time point as shown in the diagram.

To assess the expression of Gas2 during density-dependent growth inhibition, NIH 3T3 cells were seeded in 10% FCS, and every 2 d the medium was replaced with fresh 10% FCS. Gas2 increases between day 4 and 6 and continues to increase up to 8 d from seeding while the amount of both vimentin and tubulin does not change. DNA synthesis analysis shows a complete block at 4 d after seeding, concomitantly with the increased level of Gas2 expression (Fig. 2 B).

Finally serum-deprived cells were reintroduced into the growth cycle by adding 20% of FCS and Gas2 was analyzed at different times. Despite the documented down regulation of gas2 mRNA (30), the level of Gas2 remains constant, slightly decreasing only after 15 h after stimulation (Fig. 2 C).

DNA synthesis was checked by BrdUrd incorporation during the synchronous induction into cell cycle. Vimentin seems to be expressed at a constant level, whereas the amount of tubulin increases during growth induction.

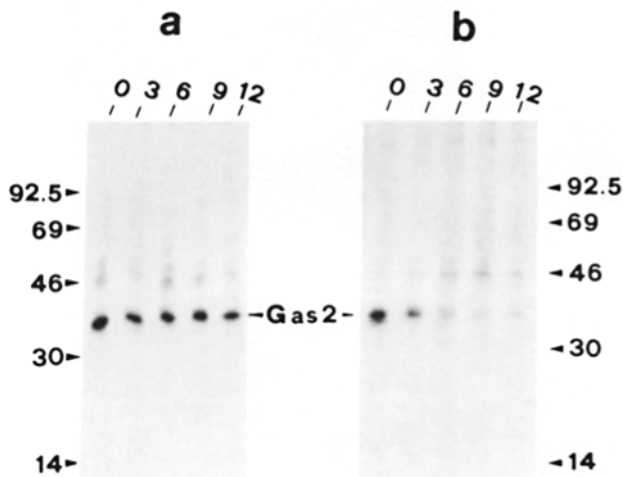


**Figure 3.** Immunoprecipitation analysis of Gas2 expression during Go→G1 transition. (a) Serum-starved NIH 3T3 cells were labeled for 12 h with [<sup>35</sup>S]methionine. 20% FCS medium containing cold methionine chase was added for the indicated times before cell lysis. Immunoprecipitations were performed using an equal number of TCA precipitable counts. (b) NIH 3T3 cells that were serum starved and activated with 20% FCS for the indicated times were labeled with [<sup>35</sup>S]methionine for 3 h before cell lysis. Immunoprecipitations were performed using same numbers of TCA precipitable counts.

#### Behavior of Gas2 during the Go→G1 Transition

The lack of “steady-state” Gas2 downregulation during the Go→G1 transition, (Fig. 2 C) appears to be in contrast with the immunoprecipitation results shown in Fig. 1 b, showing a clear downregulation in Gas2 biosynthesis 6 h after serum stimulation, together with a tight coupling of Gas2 synthesis with the Go state.

To gain further knowledge on the regulation of Gas2 in vivo biosynthesis we dissected the Go→G1 transition by a detailed immunoprecipitation analysis. NIH 3T3 cells were grown for 36 + 12 h labeling with [<sup>35</sup>S]methionine in 0.5% of FCS. 20% FCS, in medium containing a cold methionine chase, was then added to the individual dishes. After the indicated times the cells were processed for immunoprecipitation using equal numbers of TCA precipitable counts for each time point.

Fig. 3 a shows the result of such an analysis: Gas2 is detectable at a similar level at time 0 (growth arrest) and after 12 h from the addition of 20% FCS in medium containing cold methionine. Intermediate times show a similar level of Gas2 product as that at time 0. The same results were also obtained when serum-starved cells were grown for 12-h periods in the presence of 0.5% FCS and cold methionine (data not shown). This result together with Western analysis (see Fig. 2 C) indicates that the half-life of Gas2 is longer than 12 h.

Fig. 3 b represents the immunoprecipitation analysis of Gas2 from serum-starved NIH 3T3 cells, and after different times of 20% FCS growth stimulation. Cells were labeled for

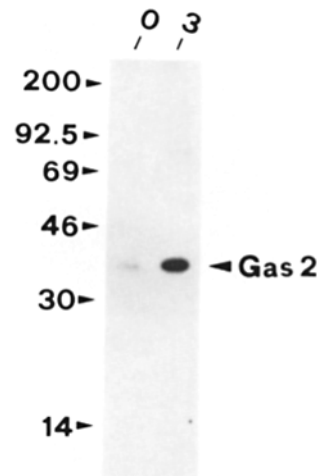


**Figure 4.** Phosphorylation of Gas2 after addition of 20% FCS to serum-starved NIH 3T3 cells. NIH 3T3 cells serum starved (0) or serum activated for 3 h (3) were pre-labeled for 8 h with <sup>32</sup>Pi. After cell lysis immunoprecipitations were performed using same numbers of TCA precipitable counts.

3 h with [<sup>35</sup>S]methionine before cell lysis, and equal amounts of TCA precipitable cpm were used for each immunoprecipitation. The amount of Gas2 protein synthesized during the first 3 h of the transition is ~50% of the protein synthesized during the Go state; but already during 3–6 h from growth induction, de novo Gas2 biosynthesis is much lower and keeps on decreasing in the following times. The analysis of Gas2 de novo biosynthesis during the Go→G1 transition thus reflects the pattern of mRNA expression.

#### Posttranslational Modifications

As the steady-state level of Gas2 does not change dramatically during the Go→G1 transition, we asked whether post-translational mechanisms might control its activity during the Go→G1 transition.

To answer this question we took advantage of the computer analysis of the gas2 cDNA sequence to screen consensus sequences for posttranslational modifications. We found two sites for cAMP/cGMP-dependent kinase, five for protein kinase C, and five for casein kinase II.

We thus analyzed the in vivo state of Gas2 phosphorylation as a function of time after serum addition. Quiescent NIH 3T3 cells were incubated in phosphate-free culture medium containing [<sup>32</sup>P]orthophosphate and 0.5% FCS for 8 h. After this labeling period the medium was either added with 20% FCS (activated cells) or left unchanged (resting cells) for a further 3 h. Equal numbers of TCA precipitable cpm were immunoprecipitated with anti-gas2 antibodies.

Fig. 4 shows that in serum-starved cells Gas2 is phosphorylated at a very low level, but it is strongly phosphorylated in cells induced into growth cycle with 20% FCS for 3 h (Fig. 4). Thus, a candidate posttranslational regulatory mechanism to control Gas2 activity is the regulation of its phosphorylation level by mitogens.

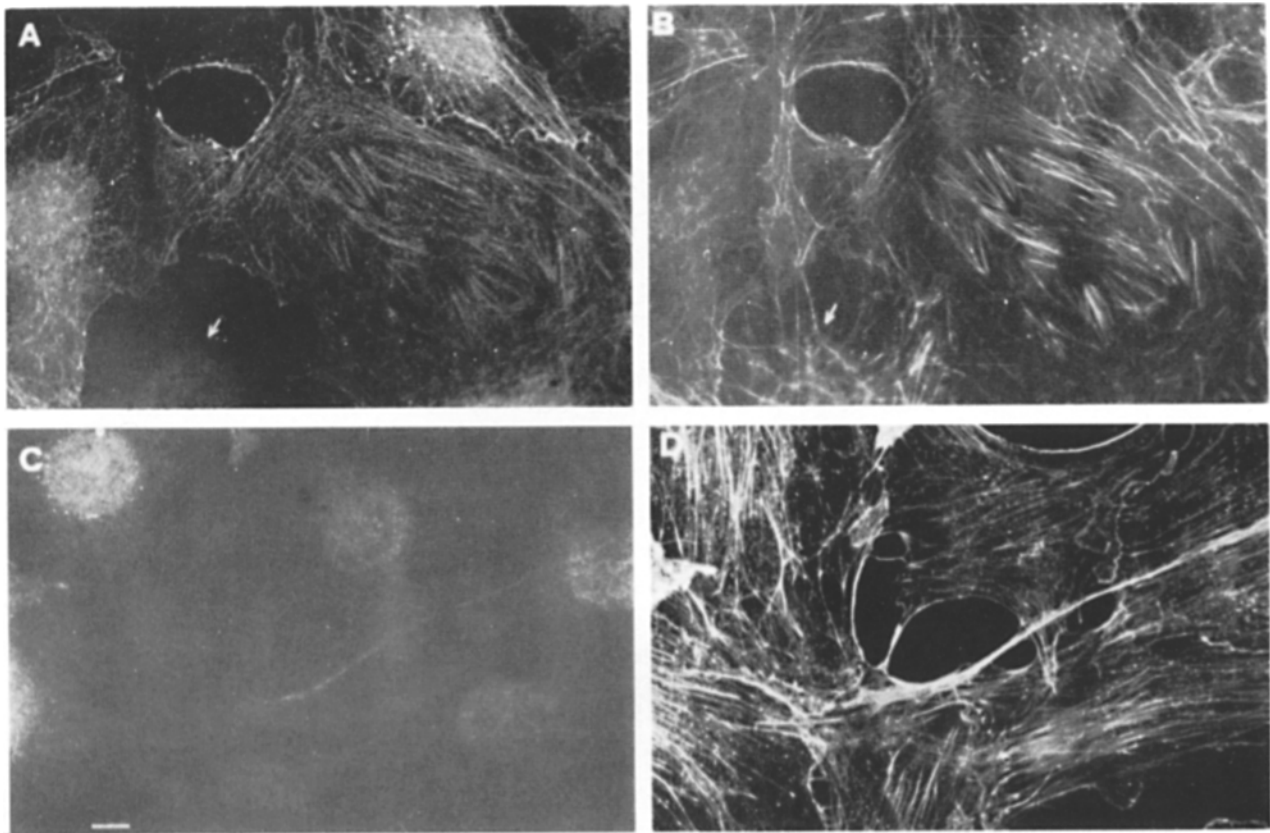


**Figure 5.** Immunofluorescence microscopy localization of Gas2, and F-actin in NIH 3T3 cells. Serum-starved cells stained with anti-Gas2 antibody (A) or phalloidin-FITC (B). Exponentially growing cells stained with anti-Gas2 antibody (C) or with phalloidin-FITC (D). Bar, 7  $\mu$ m.

### ***Intracellular Localization of Gas2***

To help understand the functional role of a protein it is important to determine its intracellular localization. We used anti-gas2 antibodies to immunostain NIH 3T3 cells under different growth conditions.

Fig. 5 A represents the indirect immunofluorescence localization of Gas2 in serum-starved cells. Cells were fixed with 3% paraformaldehyde, permeabilized with Triton X-100 and processed for immunofluorescence, (similar results were obtained after fixation in 1/1 acetone methanol).

Gas2 is present at the periphery of the cells in an area close to the cell border and along the stress fibers of actin.

An interesting observation concerns the heterogeneity of the signal: not all cells show a comparable level of intensity. Some of them are negative (Fig. 5 A, *arrow*) and some others are strongly positive, and a third type shows intermediate intensity of the signal. Fig. 5 B represents the same field stained with phalloidin-FITC to decorate the distribution of microfilaments. By a comparative analysis between Fig. 5 A and B, it can be noticed that the pattern of immunofluorescence of Gas2 resembles the pattern of distribution of the actin filaments, although actin is present in all cells, whereas some cells are negative for staining with anti-gas2 antibodies (Fig. 5 A, *arrows*).

As expected from the Western and immunoprecipitation analysis Gas2 is undetectable in exponentially growing cells (Fig. 5 C). Permeabilization of the growth-arrested cells with extraction buffer (20 mM TEA, 100 mM KCl, 2 mM

MgCl<sub>2</sub>, 0.1% Triton X-100, 1 mM PMSF) before fixation eliminated most antibody labeling at the immunofluorescence level. The loss of signal seems to be insensitive to salt concentration from 10 to 150 mM KCl and to the presence of 20% ethanediol (31) (data not shown).

These results have also been confirmed by biochemical fractionation analysis: immunoprecipitations performed from SDS or NP-40-solubilized, [<sup>35</sup>S]methionine-labeled lysates do not show any difference in the intensity of the corresponding Gas2 band (data not shown).

### ***Microinjection of GST-Gas2 Fusion Protein***

To confirm the association of Gas2 with the microfilament system, a GST-Gas2 fusion protein was microinjected in cells which normally do not express it (growing cells), and its cellular localization was followed by anti-GST antibody.

The purified fusion protein GST-Gas2 produced in bacteria was microinjected in exponentially growing NIH 3T3 cells where the amount of endogenous Gas2 is undetectable by immunofluorescence. Its pattern of distribution was followed using antibodies directed against GST, (the same results were obtained also using anti-Gas2 antibody). As a control, GST protein alone was microinjected and identified using antibodies directed against GST protein. Cells were fixed 1 h after microinjection and processed for immunofluorescence.

Fig. 6 A shows a field of cells microinjected with GST-Gas2 protein and Fig. 6 C shows the same field stained with

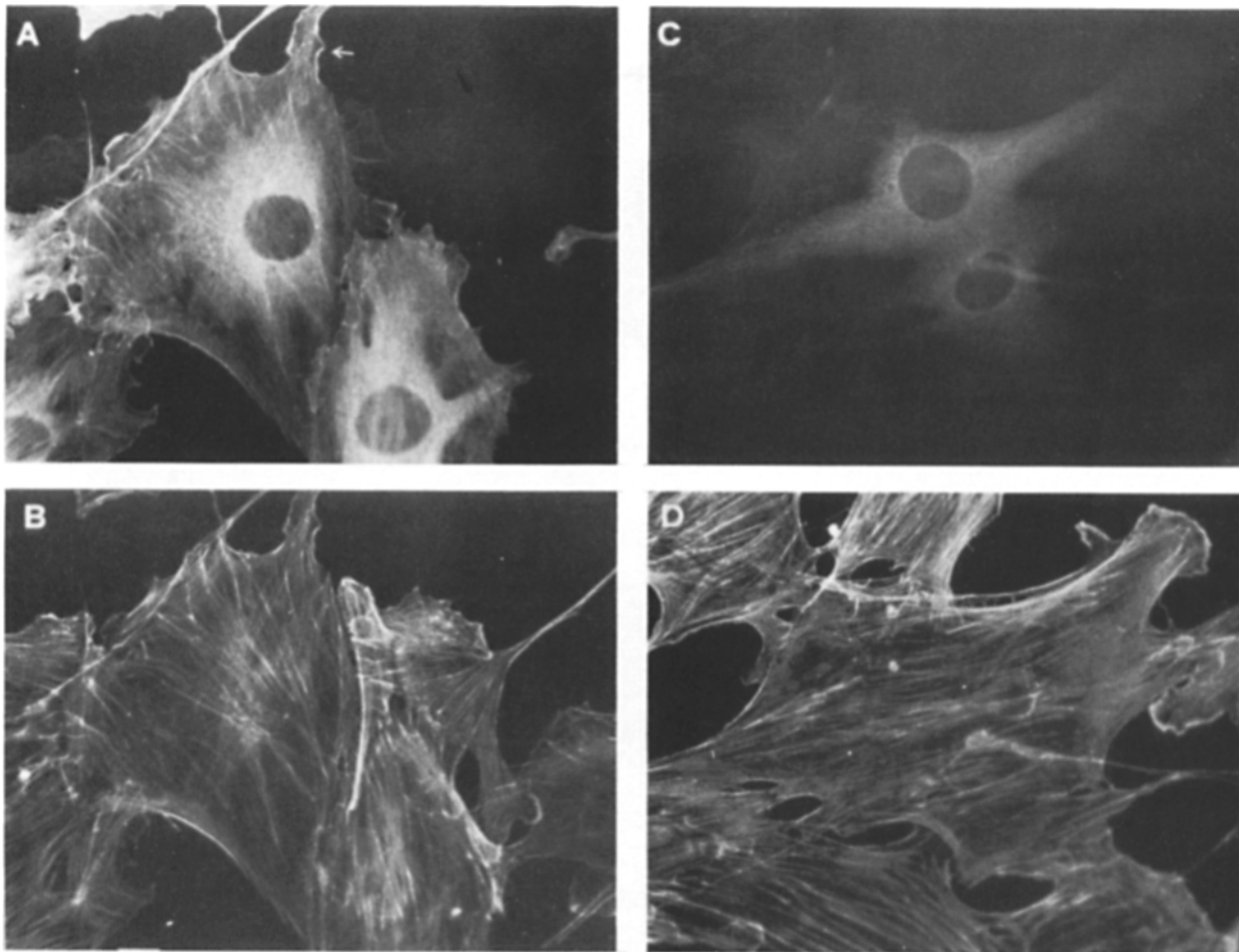


**Figure 6.** Immunofluorescence microscopy localization of GST-Gas2 fusion protein or GST after microinjection in exponentially growing cells. (A) Exponentially growing cells microinjected with GST-Gas2 fusion protein and visualized with anti-GST antibody. (*arrow* indicates cell border). (B) Same field as in A stained with phalloidin-TRITC. (C) Exponentially growing cells microinjected with GST protein and visualized with anti-GST antibody. (D) Same field as in C stained with phalloidin-TRITC. Bar, 7  $\mu$ m.

phalloidin-TRITC. Gas2 is detectable along the stress fibers and at the cell border (Fig. 6 A, *arrow*) with a distribution quite similar to endogenous Gas2 as visualized in growth-arrested cells (Fig. 5 A). The diffuse staining in the cytoplasm may be due to an excess of GST-Gas2. Fig. 6 C shows a cell microinjected with GST protein and stained with antibody specific for the GST, the same field is visualized for actin staining using phalloidin-rhodamine (Fig. 6 D). As can be seen, the GST microinjected protein is only detectable in the cytoplasm, with no staining of the actin filaments or of the cell border.

An interesting feature regarding the pattern of distribution of Gas2 emerges when it is microinjected in cells that exhibit a developed system of microvilli on the cell surface. It has been previously reported (6, 7) that NIH 3T3 cells can normally develop short microvilli on the cell surface and their appearance is favored by high cell density, reaching  $\sim$ 10–15% of population in near confluent cells.

Gas2 seems to be localized specifically in the microvilli on the cell surface (Fig. 7 A) following the pattern of the actin microfilaments (Fig. 7 B).

GST was not detectable in this structure (Fig. 7 C) even if microvilli are detectable in the microinjected cells (see

Fig. 7 D, *arrows*). We microinjected a total of 292 cells with GST-Gas2 protein and in 60 of them GST-Gas2 was preferentially localized in the microvillar structures. In the case of GST alone 242 cells were microinjected and no GST was detectable at the level of microvilli. These data thus strengthen the view that Gas2 is a component of the microfilament network system.

#### ***Analysis of Gas2 Expression in Human Diploid Fibroblasts IMR 90 and in NIH 3T3 Cells Transformed with Various Oncogenes***

To both understand the evolutionary conservation of Gas2 and its tight growth regulation with respect to other cellular systems, we performed a Western analysis on human diploid fibroblasts IMR 90 induced into growth arrest by density-dependent inhibition. IMR 90 were seeded in 10% FCS and every 2 d the medium was replaced with fresh 10% FCS. Human Gas2 is detectable as a band of 36 kD (apparent molecular mass) (Fig. 8) indistinguishable in size from the murine form, and shows a similar behavior in both IMR 90 and NIH 3T3 cells, concerning its tight association with growth arrest (Fig. 2 b). The amount of vimentin and DNA synthesis analysis are also reported.

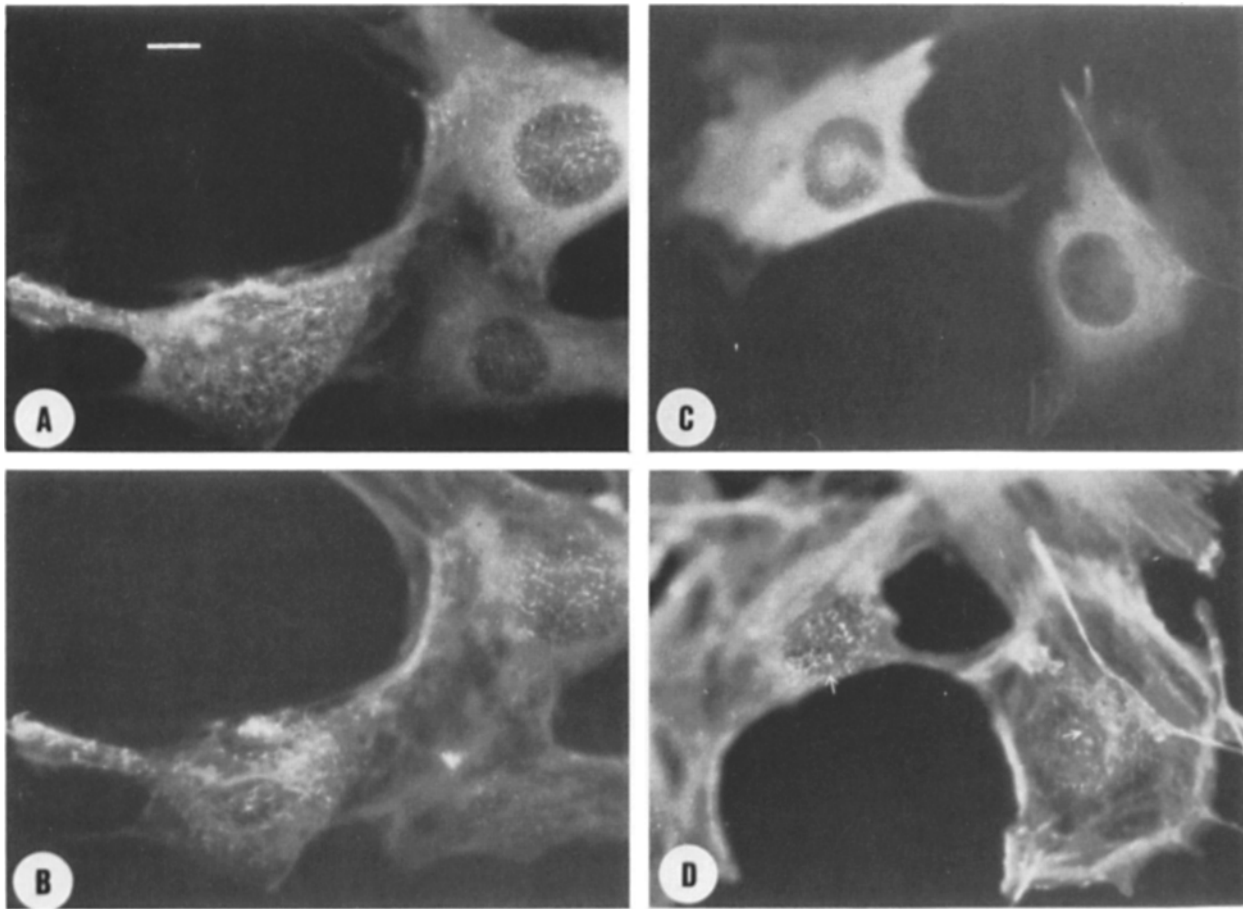


**Figure 7.** Immunofluorescence microscopy localization of GST-Gas2 fusion protein or GST after microinjection in exponentially growing cells. (A) Exponentially growing cells microinjected with GST-Gas2 fusion protein and visualized with anti-GST antibody. (B) Same field as in A stained with phalloidin TRITC. (C) Exponentially growing cells microinjected with GST protein and visualized with anti-GST antibody. (D) Same field as in C stained with phalloidin TRITC. Bar, 5  $\mu$ m.

Thus, Gas2 is a protein whose expression is coordinately regulated during growth arrest also in diploid fibroblast and evolutionarily conserved throughout species.

Cellular transformation, on the other hand, leads to alterations in cell shape, cellular metabolism, gene expression, and growth control and, as a prerogative, is defective in reaching growth arrest (17).

We thus decided to analyze the pattern of Gas2 expression in a series of single oncogene transformed NIH 3T3 cells. Fig. 9 shows such analysis: exponentially growing and serum-starved cells were used for a Western analysis. Gas2 expression increases in nontransformed cells when serum starved for 48 h. On the contrary, in all the oncogene transformed cells analyzed: (*v-fos*, *v-myc*, *v-ras*, *v-src*), the expression of Gas2 fails to increase in response to serum starvation: the amount of Gas2 protein is comparable to the amount detectable in growing cells.

### Discussion

Growth arrest, out of cycle or G<sub>0</sub> has been generally looked upon as a "negative" phase existing only in relation to the "in cycle" phase. The isolation of genes highly expressed at growth arrest (*gas*) has given credit to its existence by

providing new tools in the dissection of the cellular biology of growth arrest.

In this report we have identified, both at the biochemical and cell biological level, the product of one of these genes (*gas2*). Gas2 is present in serum-starved cells at the level of the cell border where it colocalizes with the actin fibers; it is also present, albeit at lower intensity, along the stress fibers. The interaction between Gas2 and actin filaments was strengthened by microinjection experiments.

First, we have found that Gas2, when microinjected in growing cells, has a similar distribution as the endogenous Gas2 in arrested cells. Secondly, in the same set of experiments, we have also noticed the localization of Gas2 at the level of microvilli when they are present in the microinjected cells. A very similar localization is also achieved by other, more characterized ABPs such as villin (for review see ref. 8). In fact, when villin is overexpressed in CV-1 monkey kidney fibroblasts it can localize both at the cell border and in the microvillar apparatus (7).

Prior treatment of unfixed cells with nonionic detergents determines its complete extraction: this is in accordance with its putative interaction with some components of the cellular membrane similar to what has been demonstrated for some ABPs (15). However, computer sequence analysis

DAYS AFTER SEEDING IN 10% FCS

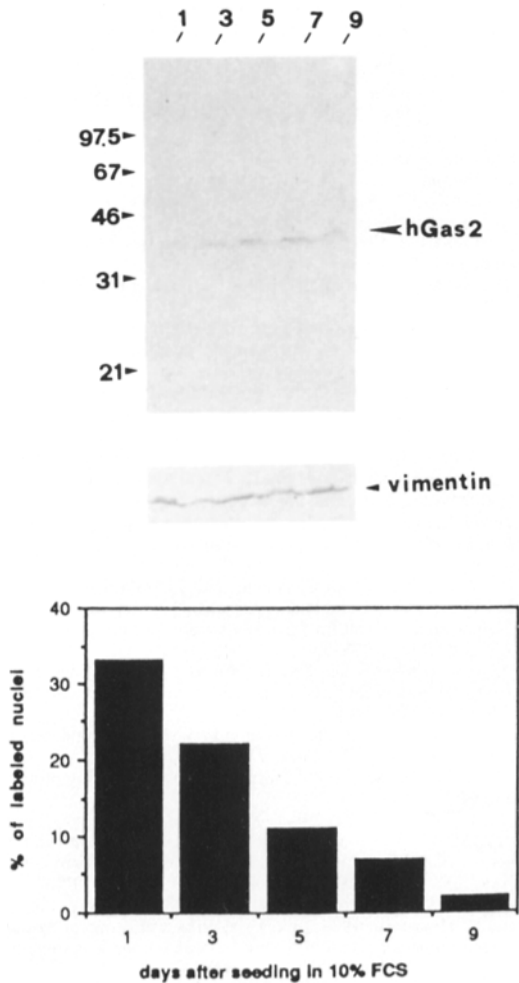


**Figure 8.** Western blot analysis of Gas2 expression in human fibroblast IMR 90. Proteins were extracted from actively growing cells and various days after cells seeding, as reported in the figure. Immunodecorations were performed with anti-Gas2 and antivimentin antibodies. BrdUrd incorporation is shown as a diagram at the bottom.

of Gas2 has not pointed out any significant homology to previously cloned ABPs or other proteins' components of the microfilament system (36). Therefore, we cannot say if Gas2 interacts directly with actin or if this interaction is mediated by other proteins (ABPs) or other factors. The availability of the GST-Gas2 fusion protein and deleted derivatives will allow us to investigate this important problem. The demonstration that GST-Gas2, microinjected into growing cells expressing an undetectable endogenous level, is able to localize in similar compartments as found in growth-arrested cells, infers that its expression is the first level for the regulation of its activity. The biochemical analysis has in fact shown that Gas2 becomes induced only at growth arrest. The apparent heterogeneity of Gas2 staining in growth-arrested cells is not inconsistent with this relation. In fact double-labeling experiments for Gas2 expression and S phase marker (BrdUrd) have revealed that the fraction of cells

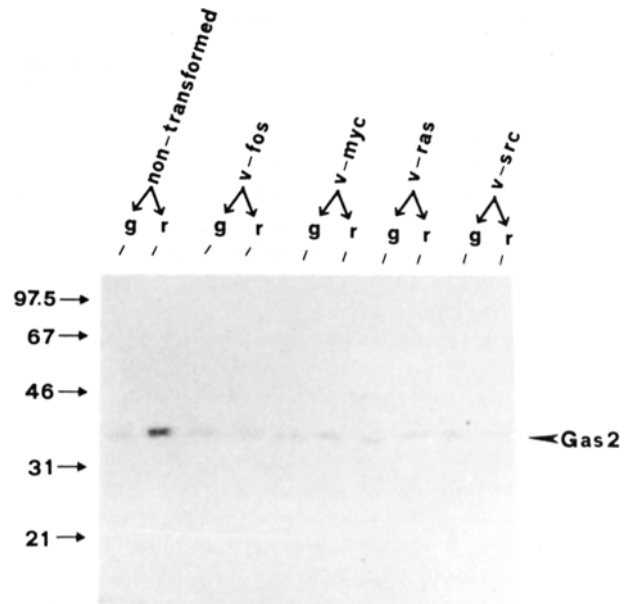


**Figure 9.** Western blot analysis of Gas2 expression in various transformed NIH 3T3 cell lines. Proteins were extracted from actively growing cells (g) or serum starved for 48 h (r) from nontransformed cells and various transformed NIH 3T3 cell lines as indicated. Equal amounts of proteins (as estimated by Coomassie blue staining of separate gels) were run on SDS/15% PAGE and blotted onto nitrocellulose.

showing stronger reactivity with Gas2 is the one with a lower number of BrdUrd-labeled nuclei, when BrdUrd labeling is performed for 14 h in 0.5% FCS (data not shown).

As Gas2 seems to have quite a long half-life, the next question to clarify was how it can be "negatively" regulated when quiescent cells are reintroduced into the cell cycle. We have in fact shown that its steady-state level does not change appreciably during Go→G1/S transition, while its de novo biosynthesis is clearly downregulated, as was expected from the mRNA expression. A clue to the putative mechanism of its regulation in the transition Go→G1/S might be a control of its phosphorylation level. Gas2 becomes highly phosphorylated after serum addition to arrested cells; a fast switch, as provided by phosphorylation rather than the regulation of its abundance level, might be more efficient in regulating its activity. Our future work will focus on the role of phosphorylation in the control of Gas2 function.

The same regulation between Gas2 expression and growth arrest is also found in other cellular systems such as IMR90 human diploid fibroblast but is dramatically perturbed in several transformed cell lines that we have analyzed. It is in fact well known that there is a tight relation between cell growth and cell shape. One of the most evident examples is the pattern of distribution of actin in transformed cells. Transformation causes a loss of stress fiber bundles of actin with a concomitant alteration in cell shape, loss of contact inhibition, and enhanced tumor-forming potential (1, 28).

Tropomyosin isoforms have been identified that are downregulated during transformation (23). More recently it has been demonstrated that gelsolin is downregulated during cellular transformation (37) and two other ABPs are also downregulated in some transformed cells (31).

Although there is evidence that some ABPs could be involved in regulating the transition shape-growth during transformation, little is known about the same changes during normal cell growth. However, it could not be misleading to hypothesize that ABPs or components of the microfilament system are involved in the regulation of actin state during different phases of cell growth. More recently a tight link between signal transduction pathways and cell shape has been demonstrated *in vitro*. Profilin (for a review see ref. 11), an ABP that inhibits the polymerization of actin monomers, binds tightly to phosphoinositol-biphosphate (18). When profilin is bound to polyphosphoinositides, it cannot bind actin monomers (18). In parallel, profilin prevents the action of phospholipase C $\gamma$ 1 on phosphoinositol-biphosphate, but *in vitro* phosphorylation of the phospholipase C $\gamma$ 1 mediated by EGF receptors can overcome the protection of the profilin on phosphoinositol-biphosphate (12).

Recently it has been demonstrated *in vivo* that the polyphosphoinositide binding profilin (19) is able to replace COOH-terminal domain mutants of CAP (38), a component of adenylyl cyclase in *Saccharomyces cerevisiae* involved in the RAS pathway (5, 10).

Thus, the identification of functions of well-characterized components of the microfilaments system has opened a new area of research in the connection between regulation of the microfilament network and cell growth. Conversely our approach, based on the identification of genes expressed in a distinct phase of cell proliferation (growth arrest), has led us to the characterization of a new component of the microfilament system that it is connected in a still undetermined way to growth control.

We would like to thank Dr. T. Kreis (European Molecular Biology Laboratory [EMBL], Heidelberg) for providing antibodies and for fruitful discussion; Prof. L. Philipson (EMBL) and Dr. M. Zanetti (University of Trieste) for carefully reading and correcting the manuscript; and the Cell Biology group at ICGEB for useful interactions.

This work was supported by Associazione Italiana Ricerca sul Cancro (AIRC) (to Claudio Schneider) as part of the special project "Oncosuppressor genes." C. Brancolini is an AIRC fellow.

Received for publication 23 December 1991 and in revised form 9 March 1992.

## References

- Boeschek, C. B., B. M. Jockusch, R. R. Friis, R. Back, E. Grundmann, and M. Bauer. 1981. Early changes in the distribution and organization of microfilament proteins during cell transformation. *Cell*. 24:175-184.
- Brancolini, C., and C. Schneider. 1991. Change in the expression of a nuclear matrix-associated protein is correlated with cellular transformation. *Proc. Natl. Acad. Sci. USA*. 88:6936-6940.
- Bretscher, A., and K. Weber. 1980. Fimbrin: a new microfilament-associated protein present in microvilli and other cell surface structures. *J. Cell Biol.* 86:335-340.
- Davis, S., M. L. Lu, S. H. Lo, S. Lin, J. A. Butler, B. J. Druker, T. M. Roberts, Q. An, and L. B. Chen. 1991. Presence of an SH2 domain in the actin-binding protein tensin. *Science (Wash. DC)*. 252:712-715.
- Field, J., A. Vojtek, R. Ballester, G. Bolger, J. Colicelli, K. Ferguson, J. Gerst, T. Kataoka, T. Michaeli, S. Powers, M. Riggs, L. Rodgers, I. Wieland, B. Wheland, and M. Wigler. 1990. Cloning and characterization of CAP, the *S. cerevisiae* gene encoding the 70 kd adenylyl cyclase-associated protein. *Cell*. 61:319-327.
- Frank, Z., M. Footer, and A. Bretscher. 1990. Microinjection of villin into cultured cells induces rapid and long-lasting changes in cell morphology but does not inhibit cytokinesis, cell motility, or membrane ruffling. *J. Cell Biol.* 111:2475-2485.
- Friederich, E., C. Huet, M. Arpin, and D. Louvard. 1989. Villin induces microvilli growth and actin redistribution in transfected fibroblast. *Cell*. 59:461-475.
- Friederich, E., E. Pringault, M. Arpin, and D. Louvard. 1990. From the structure to the function of villin, an actin-binding protein of the brush border. *BioEssays*. 12:403-408.
- Geiger, B., K. T. Tokuyasu, A. H. Dutton, and S. J. Singer. 1980. Vinculin, an intracellular protein localized at specialized sites where microfilament bundles terminate at cell membrane. *Proc. Natl. Acad. Sci. USA*. 77:4127-4131.
- Gerts, J., K. Ferguson, A. Vojtek, M. Wigler, and J. Field. 1991. CAP: a bifunctional component of the *S. cerevisiae* adenylyl cyclase-complex. *Mol. Cell. Biol.* 11:1248-1257.
- Goldschmidt-Clermont, P. J., and P. A. Janmey. 1991. Profilin a weak CAP for actin and RAS. *Cell*. 66:419-421.
- Goldschmidt-Clermont, P. J., J. W. Kim, L. M. Machesky, S. G. Rhee, and T. D. Pollard. 1991. Regulation of Phospholipase C- $\gamma$ 1 by profilin and tyrosine phosphorylation. *Science (Wash. DC)*. 251:1231-1233.
- Harlow, E., and D. Lane. 1988. *Antibodies: A Laboratory Manual*. Cold Spring Harbor Lab, Cold Spring Harbor, NY. 726 pp.
- Hartwig, J. H., and D. Kwiatkowski. 1991. Actin-binding proteins. *Curr. Opin. Cell Biol.* 3:87-97.
- Hartwig, J. H., K. A. Chambers, and T. P. Stossel. 1989. Association of gelsolin with actin filaments and cell membranes of macrophages and platelets. *J. Cell Biol.* 108:467-479.
- Kitamura, K., M. Suzuki, and K. Uyemura. 1976. Purification and partial characterization of the glycoproteins in bovine peripheral nerve myelin membrane. *Biochimica et Biophysica Acta*. 455:806-816.
- Land, H., L. F. Parada, and R. A. Weinberg. 1983. Tumorigenic conversion of primary embryo fibroblasts requires at least two cooperating oncogenes. *Nature (Lond.)*. 304:596-602.
- Lassing, I., and U. Lindberg. 1985. Specific interaction between phosphatidylinositol 4,5-bisphosphate and profilinactin. *Nature (Lond.)*. 314:472-474.
- Machesky, L., P. J. Goldschmidt-Clermont, and T. Pollard. 1990. The affinities of human platelet and *Acanthamoeba* profilin isoforms for polyphosphoinositides account for their relative abilities to inhibit phospholipase C. *Cell. Reg.* 1:973-950.
- Manfioletti, G., E. Ruaro, G. Del Sal, L. Philipson, and C. Schneider. 1989. A growth arrest-specific (gas) gene codes for a membrane protein. *Mol. Cell. Biol.* 10:2924-2930.
- Marston, F. A. O. 1986. The purification of eukaryotic polypeptides synthesized in *Escherichia coli*. *Biochem. J.* 240:1-12.
- Matsudaria, P., and P. Janmey. 1988. Pieces in the actin-severing protein puzzle. *Cell*. 54:139-140.
- Matsumura, F., J. J.-C. Lin, S. Yamashiro-Matsumura, G. P. Thomas, and W. C. Topp. 1983. Differential expression of tropomyosin forms in the microfilaments isolated from normal and transformed rat cultured cells. *J. Biol. Chem.* 258:13954-13964.
- Deleted in proof.
- Okabe, S., and N. Hirokawa. 1989. Incorporation and turnover of biotin-labeled actin microinjected into fibroblastic cells: an immunoelectron microscopic study. *J. Cell Biol.* 109:1581-1595.
- Pavalko, F. M., and K. Burridge. 1991. Disruption of the actin cytoskeleton after microinjection of proteolytic fragments of  $\alpha$ -actinin. *J. Cell Biol.* 114:481-491.
- Pepperkok, R., M. Zanetti, R. King, D. Delia, W. Ansorge, L. Philipson, and C. Schneider. 1988. Automatic microinjection facilitates detection of growth inhibitory mRNA. *Proc. Natl. Acad. Sci. USA*. 85:6748-6752.
- Pollack, R. C., M. Osborn, and K. Weber. 1975. Patterns of organization of actin and myosin in normal and transformed cultured cells. *Proc. Natl. Acad. Sci. USA*. 72:994-998.
- Schedel, T., T. G. Burland, K. Gull, and W. F. Dove. 1984. Cell cycle regulation of tubulin RNA level, tubulin protein synthesis, and assembly of microtubules in *Physarum*. *J. Cell Biol.* 99:156-165.
- Schneider, C., R. King, and L. Philipson. 1988. Genes specifically expressed at growth arrest of mammalian cells. *Cell*. 54:787-793.
- Shapland, C., P. Lowings, and D. Lawson. 1988. Identification of new actin-associated polypeptides that are modified by viral transformation and changes in cell shape. *J. Cell Biol.* 107:153-161.
- Smith, D. B., and K. S. Johnson. 1988. Single-step purification of polypeptides expressed in *Escherichia coli* as fusions with glutathione S-transferase. *Gene*. 67:31-40.
- Stossel, T. P. 1989. From signal to pseudopod. How cells control cytoplasmic actin assembly. *J. Biol. Chem.* 264:18261-18264.
- Stossel, T. P., C. Chaponnier, R. M. Ezzel, J. H. Hartwig, P. A. Janmey, D. J. Kwiatkowski, S. E. Lind, D. B. Smith, F. S. Southwick, H. L. Yin, and K. S. Zaner. 1985. Nonmuscle actin-binding proteins. *Annu. Rev. Cell Biol.* 1:353-402.
- Studier, F. W., and B. A. Moffatt. 1986. Use of bacteriophage T7 RNA polymerase to direct selective high-level expression of cloned genes. *J. Mol. Biol.* 189:113-130.
- Tellam, R. L., D. J. Morton, and F. M. Clarke. 1989. A common theme in the amino acid sequences of actin and many actin-binding proteins? *Trends Biochem. Sci.* 14:130-133.
- Vandekerckove, J., G. Bauw, K. Vancompernelle, B. Honore, and J. Celis. 1990. Comparative two-dimensional gel analysis and microsequencing identifies gelsolin as one of the most downregulated markers of

- transformed human fibroblast and epithelial cells. *J. Cell Biol.* 111: 95-102.
38. Vojetek, A., B. Haarer, J. Field, J. Gerst, T. D. Pollard, S. Brown, and M. Wigler. 1991. Evidence for a functional link between profilin and CAP in the yeast *S. cerevisiae*. *Cell.* 66:497-505.
39. Weber, K., and U. Groeschel-Stewart. 1974. Myosin antibody: the specific visualization of myosin containing filaments in non muscle cells. *Proc. Natl. Acad. Sci. USA.* 71:4561-4564.
40. Wehland, J., M. Osborn, and K. Weber. 1979. Cell to substratum contacts in living cells: a direct correlation between interference reflection and indirect immunofluorescence microscopy using antibodies against  $\alpha$ -actinin. *J. Cell Sci.* 37:257-273.
41. Welcher, A. A., U. Suter, M. De Leon, G. J. Snipes, and E. M. Shooter. 1991. A myelin protein is encoded by the homologue of a growth arrest specific gene. *Proc. Natl. Acad. Sci. USA.* 88:7195-7199.